ISSN: 2454-9940

INTERNATIONAL JOURNAL OF APPLIED SCIENCE ENGINEERING AND MANAGEMENT

E-Mail :
editor.ijasem@gmail.com
editor@ijasem.org

www.ijasem.org

INTERNATIONAL JOURNAL OF APPLIED SCIENCE ENGINEERING AND MANAGEMENT

ISSN2454-9940www.ijsem.org

Vol 5, Issuse.4 Oct 2017

A Local Metric for Defocus Blur Identification

[1]Anishetty Shiva Rama
[2]D Navya,
[3]Firdose Fathima, ,

Abstract—The challenge of detecting defocus blur in computer vision and digital image is complex and time-consuming. Designing local sharpness metric maps has been a major focus of previous work on defocus blur detection. For defocus blur detection, this research provides a simple but successful solution that relies on the feature learning of several convolutional neural networks (ConvNets). In a supervised way, the ConvNets learn the most locally important aspects of the picture at the super-pixel level. We can automatically derive the local sharpness measure by altering the principal component vector by extracting convolution kernels from the trained neural network structures and using principal component analysis. It is also recommended to use the inherent properties of the hyperbolic tangent function to fine-tune the defocus blur detection result from coarse to fine. Our suggested strategy consistently outperformed earlier state-of-the-art methods in the experiments. Defocus blur, feature learning, local sharpness matrices, ConvNets, and PCA are all terms that may be found in the index.

INTRODUCTION

D The most prevalent cause of EFOCUS blur in digital photographs is an optical imaging system that is out of focus. Imaging systems all have a fixed depth of field (DOF). Distance of focus relates to how far the camera can see around the picture plane. During the picture generation process, when the camera focuses on the object plane, and the backdrop is beyond that plane or beyond the depth of field (DOF) distance, defocus blur develops. Defocus blur is a useful tool in digital photography for narrowing down the scope of a scene's details. In order to draw the viewer's attention and accentuate the primary topic, blurring the foreground and background is a useful technique. As a result, computational image processing and scene interpretation may be hindered by a blurred backdrop. In order to identify a somewhat blurry picture, blur algorithms are used. In computer vision and digital imaging, the

Krishna,Associate Professor,
Assistant Professor,

Associate Professor

Department of CSE Engineering,
Pallavi Engineering College,
Kuntloor(V),Hayathnagar(M),Hyderabad,R.R.Dist.-50150

automatic identification of blurred picture patches is an important and demanding topic. A blur kernel is often used to suit the original picture while deblurring modern images. Using local measures, the defocused picture may be precisely divided into blurred and clear areas. A lot of effort was spent into creating local sharpness measurements in previous efforts on defocus blur detection. Local metrics may be found using a variety of methods, including the

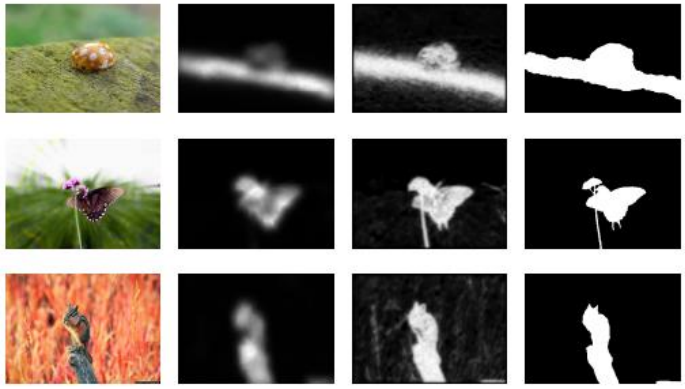

(a) (b) (c) (d)

gradient domain feature: Gradient

Figure 1 shows an example of the blur detection findings we've presented. (a) Images that have been sent in. For Alireza, the blur detection yields [37]. Images obtained by our suggested approach, with greater intensity values indicating sharper parts. Ground-truth binary maps, with white indicating sharpness and black indicating fuzziness, are shown here. As for the intensity and frequency domains, we have Histogram Span and Kurtosis, as well as Singular Value Decomposition, Linear Discriminant Analysis, and Sparsity. Lastly, we have Power Spectrum and Frequency Spectrum. The detection accuracy, detection time, and difficulty in designing blur detectors are only a few of the drawbacks of some of the suggested blur detection systems. Section II contains the most detailed information. If you don't know anything about computer vision, you can use deep learning to accomplish things like automatically identify shadows, find saliency, or partition a scene based on its semantics. Local metrics for defocus blur detection are easy, convenient, and effective. As a result, in order to identify defocus blur, we'll combine the benefits of ConvNets with a local measure. In this research, we provide a simple yet effective technique based on CNN feature learning for automatically obtaining the local metric map for defocus blur detection. This solution eliminates the need to develop time-consuming local measures and eliminates the need to have any previous knowledge of the defocused picture. We developed a new iterative updating method that takes use of the hyperbolic tangent function's inherent peculiarities in order to enhance the defocus blur detection result from coarse to fine. While the experimental results reveal that our proposed technique achieves the best possible performance and balances detection accuracy with detection time strongly, we believe that the suggested method is the best available. Fig. 1 shows the results of our suggested defocus blur detection method. Listed below are the sections of this document. Previously mentioned works are introduced in Section II. Detailed explanations of the defocus blur detection model may be found in Section III. Section IV and Section V include experiments and findings.

RELATED WORKS

It's been a two-decade-long battle to find a solution to picture deblurring. According to this prevalent belief, a blur kernel is spatially homogeneous and may therefore be inferred from global picture data. Nearly

all of these algorithms can effectively partition a blurred picture into blurred and non-blurred parts using the local metrics of image sharpness [1], [2], [4]–[7], [10], [11], [11]–[16]. As a filter function for the defocused blur picture or an energy function based on the blur's responsiveness to energy, the fuzzy regions may have a lower energy response than the sharper sections, which is why local metrics are used in this way. Recently, Liu et al. [4] proposed a technique for detecting and classifying hazy patches and pictures using four local blur parameters, including power spectrum, gradient his togram, autocorrelation congruency, and maximum saturation. But the particular kernels that influence the decrease in detection accuracy can't be estimated using this technique. In order to train a Bayes classifier for blur classification of local image areas, Shi et al. suggested a set of unique local sharpness parameters, such as gradient histogram span and kurtosis [2]. Because of its sharpness, it's considered more likely to be classed as a "sharp spot." These homogenous areas, however, are vulnerable places in their algorithm. As a result of integrating locally acquired blur evidence with globally imposed smoothness requirements, Florent et al. [10] regard blur kernel estimation as a multi-label energy reduction issue By using the picture spectrum residual [12], Tang et al. enhance the blur map from coarse to fine by utilising the inherent importance of adjacent image areas. Using the singular value decomposition (SVD) of image characteristics, Su et al. [1] offer a technique to quantify blur, and blurred areas are discovered by simple thresholding. It is proposed by Yi et al. [13] that the distribution of uniform LBP patterns in blurred and non-blurred picture areas may be used to partition defocused images. However, these systems' accuracy in detecting drugs still has to be improved. In addition to the approaches described above, several new algorithms use the local information from the frequency spectrum or magnitude spectrum to construct a blur detection sharpness measure. By studying the localised frequency spectra of the gradient field, Zhu et al. [7] attempted to explicitly estimate the space-variant PSF by taking into account smoothness and colour edge information to build a coherent blur map displaying the degree of blur at each pixel. According to Vu et al. [6], a method based on two parameters is proposed: one that takes into account local magnitude spectrum slope and another that takes into account overall variance in the area. A measurement's ultimate sharpness may be calculated by taking the geometric mean of both measurements. According to Tang et al, the connection between defocus blur and spectrum contrast at edge places may be used to estimate the blur level at the edge locations. To create a defocus map, a non-homogeneous optimization approach is used to propagate the blur amount at picture edge points. A sub-band decomposition based technique is proposed by Chakrabarti et al. in [15]. They use local frequency component analysis to estimate the probability function of a given candidate point spread function (PSF). For certain photos, their technique can identify the blur map, however their discovered maps contain locations that are wrongly labelled relative to the ground-truth. With the sparse dictionary learned from a large external collection of defocus pictures, Shi et al. [5] recommended that instead of merely judging sharpness using local information, a sparse representation of the test image patch be built. Their approach is not resilient to huge blur, since it is intended for only detectable blur estimate, thus they had to use the sparse representation of picture patches to determine how blurry the image patch was as a final assessment. Defocus blur segmentation may also be done using depth map estimation. Such approaches first estimated the amount of blur at the edge locations and then expanded the blur amount throughout the whole picture.. The defocus blur was calculated by Zhuo et al. [16] using the gradient ratios of the input and re-blurred pictures. They then used matting interpolation to extend the blur amount at the picture's edge locations throughout the whole image, resulting in a complete defocus map. The quality of the estimated blur map is strongly dependent on the precision of the edge detection and the accuracy of the blur. Despite the fact that the algorithms listed above have a chance of succeeding Image blur region detection algorithms all face difficulties in distinguishing between an in focus area and a blurred area. In addition, several of the suggested blur detection techniques still have issues, such as a low detection accuracy, a lengthy detection time, and difficulty designing a blur detector. The performance of CNNs in estimate and classification has recently been extended to blur estimation and classification. Using a convolutional neural network, Wang et al. [46] developed a classification system that can distinguish between four different kinds of pictures and then map the input images into a higher-dimensional feature space, allowing them to properly classify blurs. To estimate defocus, Jinsun Park et al. presented a convolutional neural net working structure. They used a multi-scale picture patch to extract the deep and hand-scale feature from the strong edges sparingly. A neural network classifier and a probability joint bilateral filter are used to build a sparse defocus map. Instead of using convolutional neural networks to estimate and classify defocus, as proposed by [46, 47], we want to use a different

approach. We are solely interested in using ConvNets to automatically learn the most significant characteristics in an unblurred or blurred area. [8]–[9] is also distinct from [1–7].

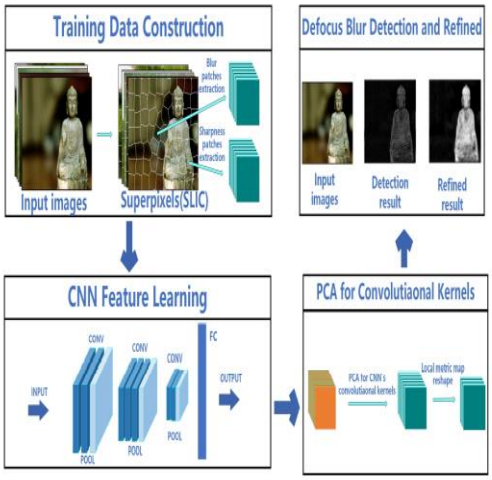

Fig. 2: The proposed defocus blur detection framework.

A lot of time and effort was invested into creating the blur detection metrics for 10], [11], [11–16]. There is no need to know any previous information about the defocused picture in order to retrieve the local measure from the trained ConvNets. An iterative approach is then developed to improve the detection outcomes. The benefits of both ConvNets and the local metric will be combined in this study to identify defocus blur. The detection precision and the detection time have been strongly balanced by us. ConvNets have a similar design to VGGs [45]. Figure 2 illustrates the suggested defocus blur detection system. Section III provides a more in-depth introduction.

PROPOSED METHOD

A number of applications, including computer vision and voice recognition, have seen considerable improvements because to deep neural networks (DNN). Convolutional Neural Networks (CNNs) are a form of DNN that has exhibited state-of-the-art results in object identification and detection in computer vision. The ConvNets architecture is being used to learn the local features of defocus blur, as well. In this research, we provide a new and easy approach for learning and extracting ConvNets features in order to acquire the local metric map for defocus blur detection. Section III contains further in-depth information on our suggested technique. Figure 2 depicts the defocus blur detection approach framework that has been presented.

The CNN-based feature learning

For a single defocused blur picture, we'll be able to pinpoint the exact location of the blur. It is possible that pixels in the unblurred region will respond strongly to local metrics such as an energy response function, which determine the label of each pixel. As a result, it is able to correctly and efficiently divide the defocused picture into blurred and clear areas. A simple yet effective framework based on the feature extraction of ConvNets is proposed in this paper for detecting blurry images. As a result, we use machine learning techniques to teach the ConvNets architecture new properties about the images. Extracting equal-sized patches around the areas of interest in the blurry or non-blurry region is used to build the ConvNets training database. Clustering homogeneous pixels into super-pixels [27] is the initial step in the extraction of local patches. Finally, a patch is retrieved by locating the centroid of each super-pixel in a ss frame. According to the hand-segmented ground truth images, we determine the category of patches by applying a threshold to the ratio of blurred or sharp regions that occupy the entire patch area, which means that there are two types of patches extracted, one from the defocus images as training data and the other from the ground truth images to determine the label of the patches extracted from the defocus images.

$$Patch = \begin{cases} blur & \text{if } \dfrac{Area_{blur}}{Area_{patch}} > T_{area} \\ unblur & \text{if } \dfrac{Area_{unblur}}{Area_{patch}} > T_{area} \end{cases}$$

where Tarea is the minimum value. Ground-truth photographs include patches with blurred or unblurred areas, which are referred to as Areablur or Areaunblur, respectively. A blur and a sharpness data collection have been compiled as a result of this research: Feature learning is accomplished by the use of a ConvNets design that employs alternating multi-convolution and sub-sampling layers, similar to the VGG architecture depicted in Figure 3 [45]. The sampling layer is connected to the multi-convolution layer through a slew of convolutional kernels. Each convolutional layer in the ConvNets architecture is used to extract feature information. Whenever size preservation was required, zero padding was applied. Two steps are taken in the sub-sampling layer to generate invariant representations from the input

feature information. To get enough kernels for convolution,

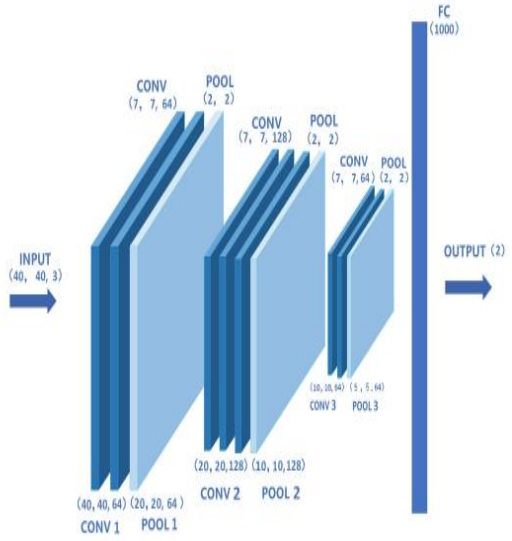

Fig. 3: The ConvNets architecture used for automatic feature learning to blurry/shapeness regions.

Convolutional layers in the deep learning network have been expanded. ConvNets may learn more hierarchical features with this multi-convolution layer topology. The last ConvNets layer is the complete connection layer, which functions as a typical Multi-Layer Perceptron with a single hidden layer. It links to the output layer. Using a logistic regression layer, the output layer produces a distribution of the classes. For the blurry and sharpness feature learning, the output layer has just two classes. ConvNets are thus based on sets of fuzzy or distinct patches. To expedite training convergence and standardise the input data, we use a batch normalisation approach. We used the CRelu [44] function as the activation function for the final complete connection layer. A supervised learning approach, ConvNetsutilises artificial neural networks. Cross-entropy loss function errors are sent into the back propagation method, which uses stochastic gradient descent to recalculate network weights. We start with a random sample from a zero-variance Gaussian distribution for the ConvNet weight. Randomly shuffled training samples allow the network to learn more quickly from unexpected examples. Heuristically, r = 0.0001 is selected as the rate at which to pick the learning rate. As a result, ConvNets are capable of autonomously learning representations for picture features. As a result, after training the ConvNets, the convolutional kernels are extracted from the architecture and processed using principal component analysis (PCA). The convolutional kernels may be analysed using principal component analysis Using principal component analysis (PCA), researchers may detect and extract vast volumes of data with various variables [31] With the use of Principal Component Analysis (PCA), data values may be distinguished from each other by how different they are from other data values. We then take the taught ConvNets architecture's convolutional kernels and dissect them. Alternating convolution and sub-sampling layers are utilised in the ConvNet architecture for feature-learning. For each layer of a ConvNets, the input feature maps are convolutioned with a bank of filter banks. Convolutional kernels are used in the filter banks. The input local maps are convolved with the convolutional kernels, which then extract the local blurry or non-blurry features. In the past, a lot of effort was invested into constructing local sharpness metrics maps or blur detection detectors for defocus blur detection. Many questions remain, though. Are there any picture attributes that determine the qualities of the image's local area: blur or sharpness?? These details may be gleaned from photos that have been locally blurred. If this is the case, how can these characteristics be obtained and reshaped into a blur detecting sensor? There is a presumption that follows: A blur detector and these characteristics exist. Primarily we may get the local sharpness metric map or blur detection detector by extracting and using principal component analysis to process convolution kernels obtained from previously trained neural networks. We take the convolution kernel out of the learned convolutional neural network structure. Convolution kernels are concatenated into a matrix, and Main Component Analysis (PCA) is used to extract the matrices' principal components. Final step: Reconstruct the main component vector whose greatest explained variance ratio we've just found! There are N convolution kernels retrieved from the trained ConvNets architecture, for example, if the convolutional kernel size is 7 x 7 and there are N convolution kernels. In other words, the size of the convolutional kernel matrix is 49N, whereas the size of the PCA matrix after dimension reduction is 49K.

C. Local metric map detection and detection results refined

In order to process the convolution kernels extracted from the trained Con vNets architectures, we use PCA. For the previous phase, we acquired K local metric maps. K = 2 indicates that two local metric maps, K1 and K2, have been remodelled, based on the contribution rate of the primary component and people's empiricism. We utilise a simple method to

identify defocused blur, like follows:

$$L_1 = Conv(\ \mathrm{I},\ K_1)$$

$$L = Conv(\ L_1,\ K_2)$$

The convolutional filter for the input picture is denoted by the function Conv(.). The defocused picture, L1 and L, represent the results of the local metric detection. It is necessary to establish an optimization strategy when detection results do not match our expectations or do not perform better. By using this inherent quirk of the hyperbolic tangent function, a new iterative updating technique is provided to enhance the defocus blur detection result from coarse to fine (tanh). Use of the tanh function in neural computation is widespread.

Algorithm 1: Iterative refinement of detection results Let Input signify L's blur detection result, and Output the iterative refined result. Using the histogram distribution of Input, determine Th that denotes the first threshold value.2

$$T_h = 1 - \frac{\sum_{i=1}^{k} h_n(i)}{\sum_{i=1}^{n} h_n(i)}$$

where n represents the total number of histogram gray levels and k represents the kth gray level of histogram

Let T_g denote the the global threshold and N de the total iterative updating numbers

Filtering $Input$ by apply the threshold T_h

repeat

  for *Each pixel i in Input* **do**

    Calculate M that denote the 3×3 neighborhood mean value of pixel i

    if $M < T_g$ **then**

      $Output(i) = 0$

    end

    if $M \geq T_g$ **then**

      $Output(i) = \frac{e^{M} - e^{-M}}{e^{M} + e^{-M}}$

    end

  end

  $Input = Output$

until *the iterative numbers* $\leq N$;

return $Output$

Activation function of network structure. This function's output values can only fall within the range of [-1,1] since it is non-linear and grows in a strictly monotonic manner. Any time the input value is more than zero, the return value will always be smaller. The tanh function's features have helped us improve our defocus blur detection findings. For the defocus blur detection, we employed an iterative update approach. Insight intoresult is a gray value image, where the unblurred regions have higher intensities hazy ones and pixel values that fall within the range [0, 1]." The revised mechanism's goal is to make the unblurred zone more responsive while decreasing the responsiveness in the blurred region. Algorithm 1 produces zero as an output when neighbourhood means are smaller than the global threshold, which always happens in the hazy area. It is only in the non-blurred area that the tanh function is used to compute the output if the neighbourhood means are larger than or equal to the global threshold. The output value of the tanh function is always smaller than the input value when the input value is greater than zero. Many pixels in the blurred area are filtered by the global threshold, which indicates that the neighbourhood means of the other pixels will be smaller in the following iteration, thus those pixels may also be filtered. As a result, it takes several iterations to get to the point of having a sophisticated mechanism. Algorithm 1 explains the method in further depth. The initial threshold Th and the global threshold Tg are used in the iterative refinement process. Using the histogram of the detection result, only the first threshold Th is automatically determined (see Algorithm 1). It's possible that certain pixels in an otherwise clear area may be filtered out because of the continual refinement of detection findings. As a consequence, we integrate the improved findings BN1, BN2, BN3 into an overall defocused blur detection result:

$$I = \prod_{i=1}^{3} B_{N_i}^{\alpha_i} \qquad (\alpha_1 + \alpha_2 + \alpha_3 = 1)$$

where $0 \leq \alpha i \leq 1$, Ni denote the number times of iterative refined, I denote the final detection result of defocus blur

EXPERIMENTAL RESULTS

Our suggested approach is evaluated here, and the outcomes of the experiments are shown. Publicly available blurred picture datasets, including 704 partly blurred photos and associated hand-segmented ground truth images, were used to evaluate the suggested approach The approach outlined in Section

III was used to segment each picture into crisp and blurred sections. Our method's blur detection findings are grayscale pictures with pixel values between [0, 1] for the time being.

Datasets

A random selection of 200 partly defocused blurred photos from the public collection was utilised in this study. The unblurred area in the ground-truth picture has an uneven form. In order to get as many boundaries as possible between the blurred and non-blurred areas, we marked the threshold of the size of blurred or sharp regions that fills the whole patch area. 0.8 = the area of the rectangle. The 4040 patch at the centroid of each superpixel was retrieved, as illustrated in Figure 4, by clustering the homogeneous pixels and denoting s = 40. Hence, the training datasets that are smudged or crisp are a result of construction.

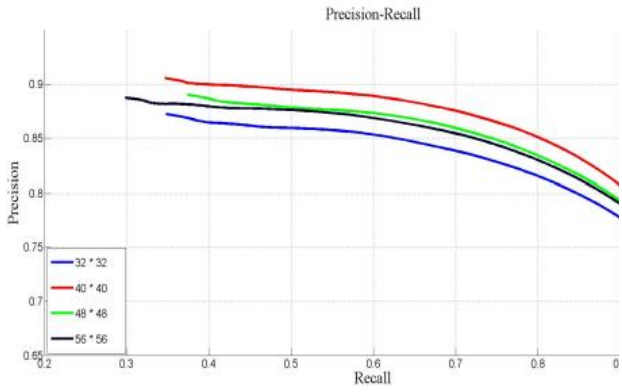

Fig. 4: The comparison of precision-recall curves for the different patches size with same convolutional size: 7×7, same global threshold: Tg = 0.005, same parameter combinations: α1 = 0.3, α2 = 0.2, α3 = 0.5.

Table 1 RUNNING TIME COMPARISON OF OTHERS DETECTION METHODS.

Methods	Chakraburti [15]	Liu [4]	shi14 [2]	shi15 [5]	Tang [11]	Alireza [37]	Su [1]	Zhou [16]
Code	matlab	matlab	matlab& cex	matlab& cex	matlab	matlab	matlab	matlab
Avg. Running Times(s)	5.2	273.19	1083.5	37.0	4.8	165.3	15.3	19.16

Experimental results

Figure 3 shows the three alternating convolution and three sub-sampling layers of the ConvNet architecture used for feature learning. The size of the convolution kernel in the multi-convolution layers of the trained ConvNets architecture is indicated as 7x7. The trained ConvNets design has seven convolution layers. The convolutional kernel matrix is constructed by extracting the convolutional kernels from the learned convolutional layers. Defocus blur is detected by reducing the matrix dimension using PCA and reshaping it to identify the picture. k = 1 and n = 4 are used in the process of determining the initial threshold Th and the global threshold Tg = 0.005 (NB. this threshold is the local mean threshold in the 33 neighbourhood. The picture has a pixel value between [0, 1] and is grayscale.) and the number of iterations N is equal to 100 Denote N1 = 10, N2 = 50, N3 = 100 and 1 = 0.3, 2 = 0.2, 3 = 0.5 throughout the iterative refinement of detection findings. Refinement of detection findings is shown in Figure 5. Our suggested method's final findings display in the rightmost columns. A total of eight current comparator techniques were compared with our algorithm [1], [2], [4], [5], [11], [15],[16], [37]. The unblurred portions have a greater intensity than the blurred ones in the comparison figure of the findings supplied. An increase in intensity suggests a sharper picture in all of these techniques' outputs. Figure 7 shows instances of detection outcomes for each method as shown by the sharpness maps. The blur map may be recognised by algorithms [1], [2], [4], [5], [37] for certain pictures, however their discovered maps contain wrongly labelled areas when compared to the ground truth. Furthermore, the blur was completely missed by algorithms [11], [15], and [16].

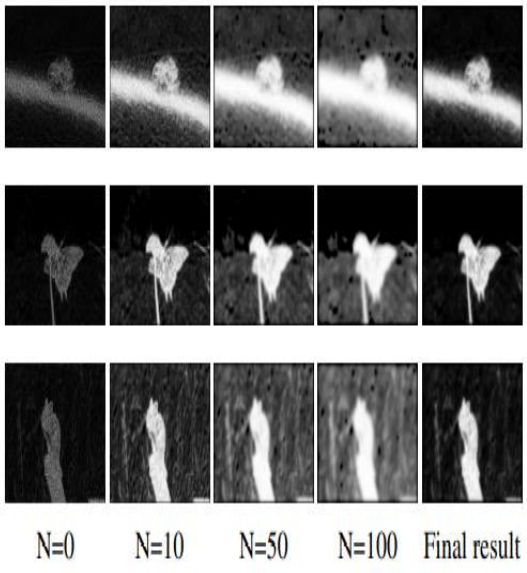

Fig. 5: The iterative updating detection results, where N denote the iterative numbers of result refined. The final results show in the rightmost cols.

To the extent that certain blurred pictures cannot be identified entirely, for single photographs. Our technique, on the other hand, is flexible enough to deal with a variety of defocus blur circumstances

while still achieving the best levels of accuracy throughout the whole recall range [0, 1]. By altering the threshold used to segment the final sharpness maps, we were able to build precision and recall curves for each algorithm.

$$\text{precision}=\frac{R\cap R_g}{R},\qquad \text{recall}=\frac{R\cap R_g}{R_g}$$

the segmented blurred region's pixels are represented by R, while the true blurred region's pixels are represented by Rg. The blur detection findings were binarized by altering the threshold between [0, 255] in this article. This method's precision-recall curves are shown in Figure 6 (a), which gives a quantitative assessment of our approach. The adaptive threshold is used to segment the binarized findings for the blur detection maps in this experiment. It is clear that our technique is better since it obtains the greatest accuracy throughout almost the whole recall range [0, 1]. To compare the precision-recall curves for various convolution kernel sizes in our trained ConvNets, as well as between unrefined and refined detection results, see Figure 6 (b). We can calculate the size of the convolution kernel needed to detect defocus blur in a single picture using these results, and we can also demonstrate the effectiveness of iterative optimization. Our detecting technique has various parameters. We ran a slew of tests in an effort to nail down the perfect set of parameters. The comparison of precision-recall curves for various global thresholds employed in iterative refinement of detection results is shown in Figure 6 (c). Figure 6. We arrived at the global threshold value based on these curves. After combining the numerous parameter combinations shown in Figure 6 (d), we were able to find the optimal performance settings for detecting defocus blur. Additionally, our technique is time-saving. The iterative sharpness metric detection using the hyperbolic tangent function consumes the greatest computing time in our approach, but there are also certain performance benefits over other techniques. Table I shows a run-time comparison of the various blur detection techniques. An Intel Core i5 4200 desktop computer with a 2.50 GHz dominant frequency and 8 GB of RAM is used for experiments. We use the authors' implementations for everything else. Tensorflow was used to train the ConvNets architecture, while Matlab was used for the run-time test of our technique. The test picture has a resolution of 640 x 457 pixels. Our project website has the source code for our work:

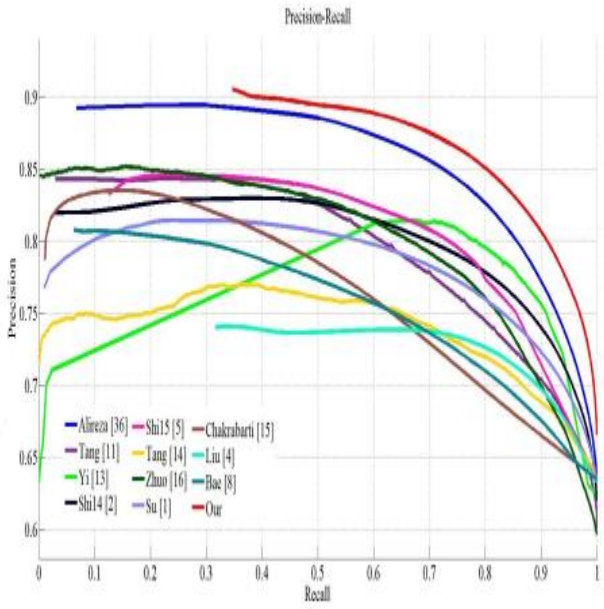

(a) The comparison of precision-recall curves for different methods.

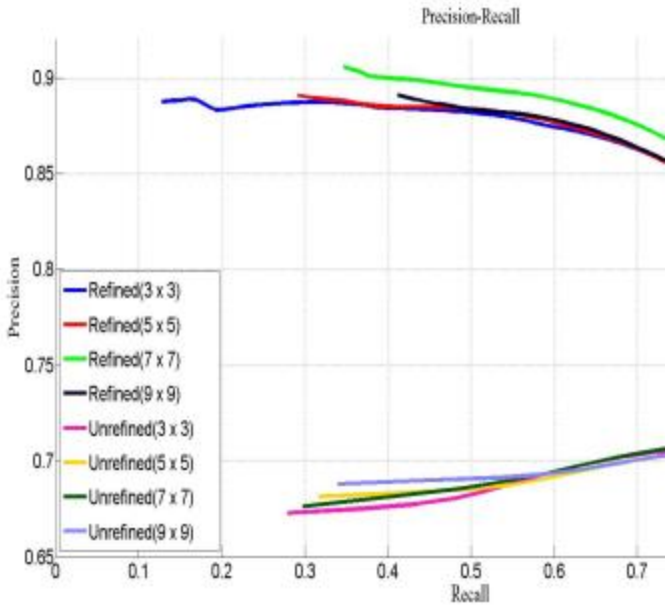

(b) The comparison of precision-recall curves for the different convolution kernel size of our trained ConvNets and the comparison of precision-recall curves between the unrefined and refined of detection results.

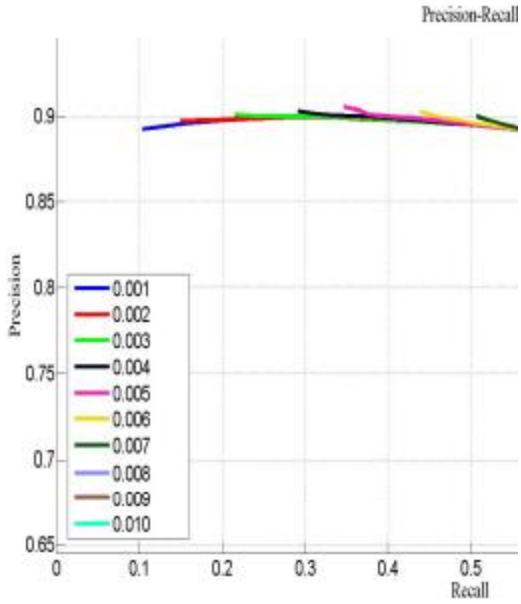

(c) The comparison of precision-recall curves for the different global threshold value of the process of detecion results refined.

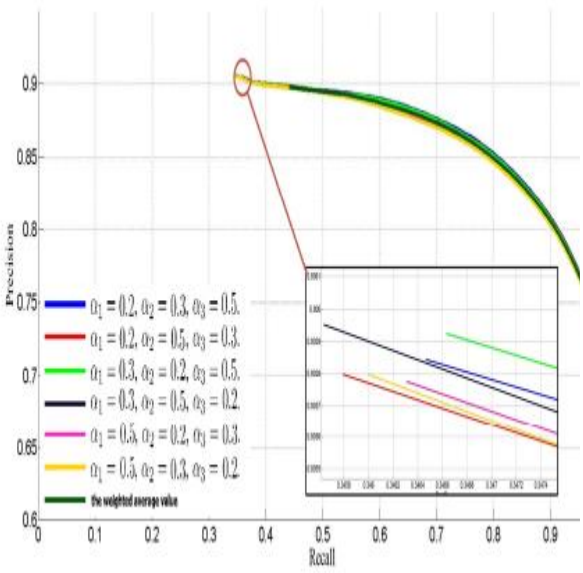

(d) The comparison of precision-recall curves for different parameter combinations of the overall perceived defocus blur detection result.

Fig. 6: Quantitative Precision Recall comparison for different methods or parameters

CONCLUSION

While defocus blur detection is an extremely difficult issue, this study proposes an innovative but successful approach that uses a CNN-based feature learning in the blurred and non-blurred parts of an image to identify defocus. It is also recommended to use the inherent oddity of the hyperbolic tangent function to improve the defocus blur detection result from coarse to fine. The results of our experiments suggest that our system can recognise defocused fuzzy images with the best accuracy in the industry.

ACKNOWLEDGMENTS

ACKNOWLEDGMENTS Jianping Shi's dataset for blur detection has been made publicly accessible as a result of the authors' gratitude. They'd also want to express their gratitude to [5] [11] [16] [37] for

making theircodepubliclyavailable.

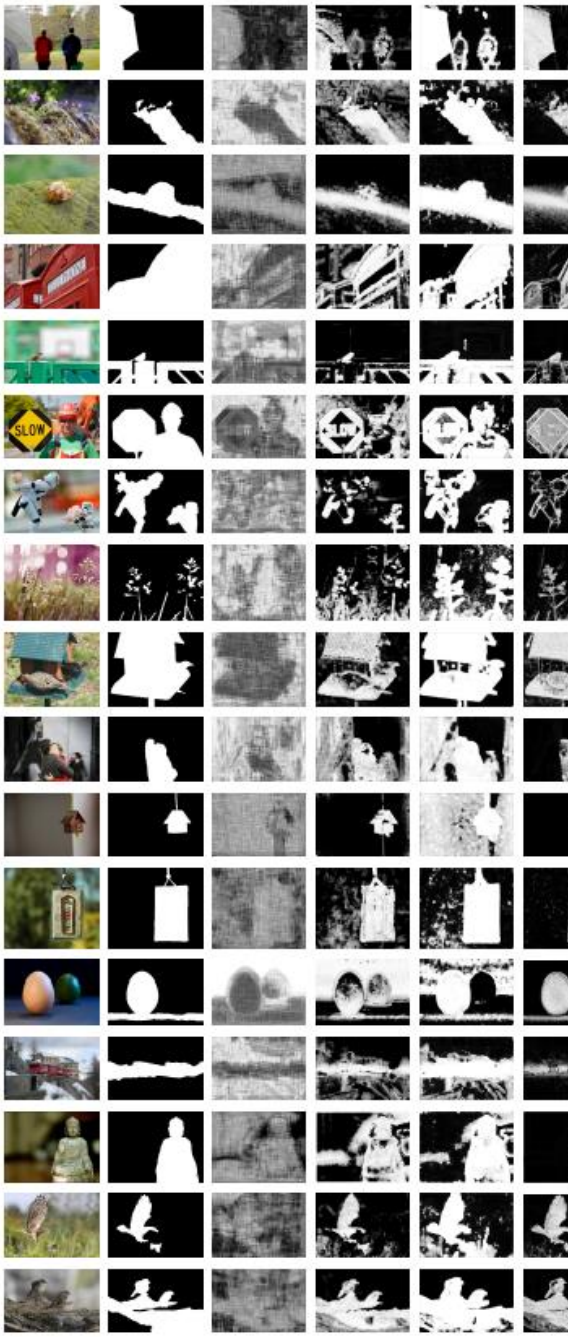

Input GT (a) (b) (c) (d) (e) (f) (g) (h) (i)

Unblurred areas seem to be brighter than blurred ones in Fig. 7, which shows results from several blur detection algorithms. Adaptive thresholds applied to the rightmost columns reveal our suggested method's segmentation outcomes. Both Zickler [15] and Liu [4] are mentioned. The Shi14 [2] [3] Finally, Shi15 [5].' The author Tang [11] Alireza [37] is the name of the protagonist. Su [1]. The name (h) is Zhuo. I We're talking about you, sir.

REFERENCES

[1] B. Su, S. Lu, and C. L. Tan, "Blurred image region detection and classification," in International Conference on Multimedea 2011, Scottsdale, Az, Usa, November 28 - December, pp. 1397–1400, 2011.

[2] J. Shi, L. Xu, and J. Jia, "Discriminative blur detection features," in Computer Vision and Pattern Recognition, pp. 2965–2972, 2014.

[3] J. Caviedes and S. Gurbuz, "No-reference sharpness metric based on local edge kurtosis," in International Conference on Image Processing. 2002. Proceedings, pp. III–53–III–56 vol.3, 2002.

[4] R. Liu, Z. Li, and J. Jia, "Image partial blur detection and classification," in Computer Vision and Pattern Recognition, 2008. CVPR 2008. IEEE Conference on, pp. 1–8, 2008. [5] J. Shi, L. Xu, and J. Jia, "Just noticeable defocus blur detection and estimation," in Computer Vision and Pattern Recognition, pp. 657–665, 2015.

[6] C. T. Vu, T. D. Phan, and D. M. Chandler, "S3: a spectral and spatial measure of local perceived sharpness in natural images," IEEE Transactions on Image Processing, vol. 21, no. 3, pp. 934–45, 2012.

[7] X. Zhu and S. e. a. Cohen, "Estimating spatially varying defocus blur from a single image," IEEE Transactions on Image Processing, vol. 22, no. 12, pp. 4879–4891, 2013.

[8] S. Bae and F. Durand, "Defocus magnification," Computer Graphics Forum, vol. 26, pp. 571–579, 2007.

[9] J. Bardsley and S. e. a. Jefferies, "A computational method for the restoration of images with an unknown, spatially-varying blur," Optics Express, vol. 14, no. 5, pp. 1767–82, 2006.

[10] F. Couzini-Devy and J. e. a. Sun, "Learning to estimate and remove non-uniform image blur," in Computer Vision and Pattern Recognition, pp. 1075–1082, 2013.

[11] C. Tang and J. e. a. Wu, "A spectral and spatial approach of coarse-tofine blurred image region

detection," IEEE Signal Processing Letters, vol. 23, no. 11, pp. 1652–1656, 2016.

[12] S. Lee, "Time-of-flight depth camera motion blur detection and deblurring," IEEE Signal Processing Letters, vol. 21, no. 6, pp. 663–666, 2014.

[13] X. Yi and M. Eramian, LBP-Based Segmentation of Defocus Blur. IEEE Press, 2016.

[14] C. Tang, C. Hou, and Z. Song, "Defocus map estimation from a single image via spectrum contrast.," Optics Letters, vol. 38, no. 10, p. 1706, 2013.

[15] A. Chakrabarti, T. Zickler, and W. T. Freeman, "Analyzing spatially

[16] S. Zhuo and T. Sim, "Defocus map estimation from a single image," Pattern Recognition, vol. 44, no. 9, pp. 1852–1858, 2011.

essing, pp. 1777–1780, 2010.

[17] M. Elad and M. Aharon, "Image denoising via sparse and redundant representations over learned dictionaries.," IEEE Transactions on Image Processing, vol. 15, no. 12, pp. 3736–3745, 2006.

[18] A. Chakrabarti and T. Zickler, Depth and Deblurring from a SpectrallyVarying Depth-of-Field. Springer Berlin Heidelberg, 2012.

[19] S. Dai and Y. Wu, "Removing partial blur in a single image," in Computer Vision and Pattern Recognition, 2009. CVPR 2009. IEEE Conference on, pp. 2544–2551, 2009.

[20] Y. W. Tai and M. S. Brown, "Single image defocus map estimation using local contrast prior," in IEEE International Conference on Image Proc